Characterization of fly-ash using electrochemical impedance spectroscopy

Available online at www.sciencedirect.com

ScienceDirect

Procedia Engineering 171 (2017) 705 – 714

Procedia Engineering

www.elsevier.com/locate/procedia

Sustainable Civil Engineering Structures and Construction Materials, SCESCM 2016

Characterization of fly-ash using electrochemical impedance spectroscopy

Benny Suryanto[a], W. John McCarter[a,*], Gerry Starrs[a], T. Malcolm Chrisp[a]

[a]*School of Energy, Geoscience, Infrastructure and Society, Heriot-Watt University, Edinburgh EH14 4AS, Scotland,UK*

Abstract

Electrochemical impedance spectroscopy is used to obtain the electrical properties of fly-ash over the frequency range 100Hz-10MHz. A range of presentation formalisms are exploited to characterize and assess this material in terms of its unburnt carbon content and pozzolanic reactivity. Fly-ash from a number of power stations within the UK, which differ in carbon content and fineness are used within the experimental programme. It is shown that the methodology could be exploited to index both the pozzolanicity and the presence of carbon in the ash. A number of additional features make this testing methodology of interest: the method is non-destructive and non-invasive; samples need not be restricted to cement pastes as mortars and concretes can also be studied.

Peer-review under responsibility of the organizing committee of SCESCM 2016.

Keywords: Fly-ash; Carbon; Pozzolanicity; Monitoring; Electrical properties.

1. Introduction

The use of alternative cementitious binders, whereby Portland cement is partially (or even totally) replaced by the by-products of traditional industries, have an important role to play both in the design of durable cementitious systems and also in the reduction of CO_2 emissions. Because of the quantities of concrete produced world-wide, even a small reduction in CO_2 emission can result in significant environmental benefits. It is incumbent upon all nations to reduce total CO_2 emissions and contribute to achieving the targets initially set at the Kyoto Conference in 1997 and reaffirmed at the more recent UN Climate Change Conference in 2015 in Paris. For the foreseeable future,

* Corresponding author. Tel.: +44-131-451-3318; fax: +44-131-451-4617.
E-mail address: w.j.mccarter@hw.ac.uk

Peer-review under responsibility of the organizing committee of SCESCM 2016.
doi:10.1016/j.proeng.2017.01.414

extensive use will be made of materials such as ground granulated blast-furnace slag, micro-silica and fly-ash. Characterization of these materials is thus of considerable importance because the amount and quality of the replacement added to the binder are, ultimately, decisive parameters in concrete performance.

The two most important factors which determine the suitability of fly-ash are its fineness (45μm residue), to ensure reactivity, and its free carbon content which is quantified by the loss-on-ignition (LOI). In the case of low-lime fly ashes produced from anthracitic and bituminous coals, the cellular nature of the carbon particles results in a high specific surface area which can adsorb significant quantities of chemical admixtures. This can have a direct influence on the effectiveness of air-entraining agents, water-reducing admixtures and retarders; furthermore, the higher the carbon-content of the ash, the higher the water demand to maintain workability. There is also scope for direct activation of fly-ash to produce construction materials requiring lower strengths, for example, masonry mortars, grouts, backfill, non-clay bricks or slurry trench cut-off walls for containment purposes. This would further increase their utilization, particularly those fly-ashes which would not satisfy BS EN450 [1] code requirements as contributing towards all (or part) of the cementitious component.

In this paper, electrochemical impedance spectroscopy (EIS) is used to study fly-ash binders; more specifically, it is shown that EIS techniques could be developed as a *signature* for fly-ash and in the study of the pozzolanicity of fly-ash by direct chemical/thermal activation thereby extending previous work [2−3].

1.1. Electrochemical Impedance Spectroscopy

The electrical response of a saturated porous material can be quantified in terms of its resistance (or its reciprocal, conductance) and capacitance. Monitoring these intrinsic electrical parameters as a function of frequency of applied electrical field represents the area of EIS. The underlying mechanisms responsible for impedance behaviour are directly related to the physical and chemical properties of the material – the capacitance is a quantitative measure of the polarization of charges within the material, and the conductance accounts for any direct transfer of charge through the material (i.e. ionic conduction) together with the dissipation of energy incurred due to relaxation of polarization processes.

The complex impedance, $Z^*(\omega)$, of a porous, ionic conductor at any angular frequency, ω, of applied electrical field, can be represented by the equation [4],

$$Z^*(\omega) = Z'(\omega) - iZ''(\omega) \tag{1}$$

where $Z'(\omega)$ and $Z''(\omega)$ represent, respectively, the resistive (or in-phase component) and reactive (or quadrature component) of the complex impedance and $i = \sqrt{-1}$. Both these components can be monitored as a function of frequency of applied field and values presented on a Nyquist plot, i.e. values $Z'(\omega)$ vs. $-iZ''(\omega)$. These are the basic concepts involved in impedance spectroscopy, with the frequency range over which measurements are made extending over several decades. A typical response for a hardened concrete is presented in Fig. 1(a) over the frequency range 100Hz-10MHz with frequency increasing from right to left across the curve [5]. The Nyquist plot comprises two distinct regions, a high frequency, bulk arc whose centre, C, is depressed below the real axis and a low-frequency spur representing the response from the electrode/sample interface. The true bulk resistance of the sample, denoted R_b, is obtained at the cusp-point between the bulk arc and low-frequency spur shown schematically in Fig. 1(b). In this paper, use is made of both the Nyquist and bulk resistance presentation formalisms.

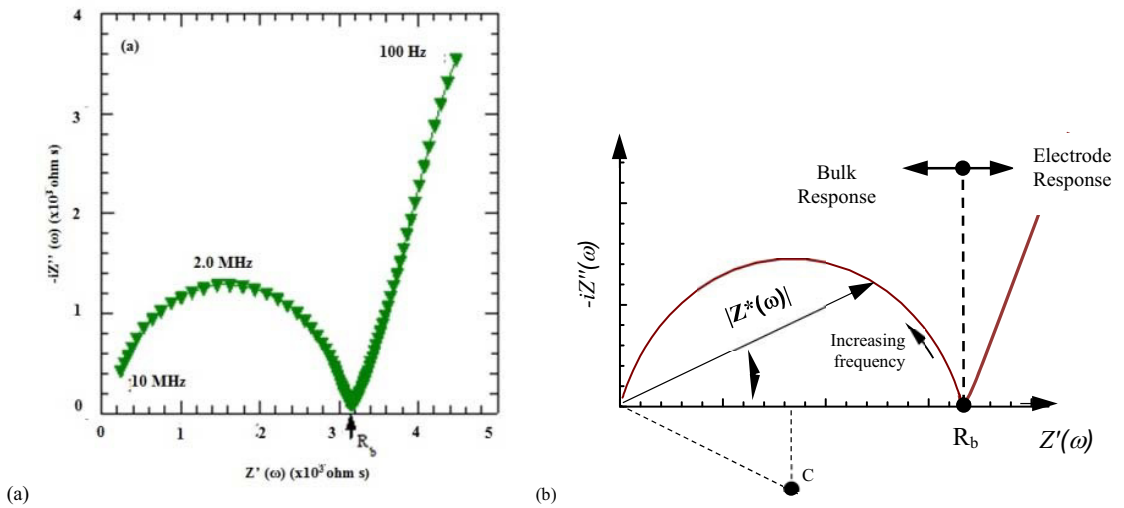

Fig. 1. (a) A typical Nyquist plot for hardened concrete, and (b) schematic showing electrode and bulk response and location of bulk resistance, R_b.

2. Experimental programme

2.1. Impedance measurements

The EIS characterization studies were developed on two fronts:
(i) Frequency-effect. In this phase of the work, EIS measurements were obtained on both the fresh (i.e. plastic) and hardened samples using a Solartron 1260 frequency response analyser (FRA) with measurements presented in the form of equation (1) above.
(ii) Pozzolanicity/Activation. Within this phase of the work, fly-ash was mixed with an activator and the electrical response monitored using an Agilent 4263B LCR meter. Measurements were undertaken at a fixed frequency of applied electrical field.

Both the FRA and LCR meter operated in voltage-drive mode with a signal amplitude of 100mV used throughout. FRA measurements were obtained over the frequency range 100Hz-10MHz using a logarithmic frequency sweep with 20 spot frequencies per decade. The LCR meter was programmed to operate at a fixed frequency of 10kHz which was optimised through EIS measurements to ensure that electrode polarization effects had a negligible influence on evaluation of R_b (see Fig. 1(b)). Connections to the FRA and LCR meter were by means of individually screened coaxial leads with measurements taken every 10 minutes over periods extending up to 150 hours. Lead inductive effects were *nulled* from the data at each measurement frequency utilising an open-circuit, short-circuit and load calibration algorithm.

2.2. Test cells, materials and sample preparation

Paste and mortar samples were compacted into rigid, sealed Plexiglas cells. The cells had internal dimensions 5×5×5cms with electrical contact established by means of 5×5×0.3 cm (thick) stainless steel electrodes attached to two opposite cell walls. For concretes, the test cell had internal dimensions 15×15×15cms with electrical contact established by means of 15×15×0.3 cm (thick) stainless steel electrodes.

Table 1: Chemical and physical properties of fly-ashes used within the experimental programme

Oxide%	FA1	FA2	FA3	FA4	FA5	FA6
SiO_2	46.5	51.0	50.5	49.6	48	44.3
Al_2O_3	28.2	27.4	24.7	25.3	27	24.7
Fe_2O_3	4.9	4.6	7.4	10.3	9	9.2
CaO	3.3	3.4	2.6	2.0	3.3	5.9
MgO	1.2	1.4	1.5	1.9	2.0	1.9
SO_3	1.09	0.7	0.8	0.77	0.6	0.69
TiO_2	1.3	1.6	1.0	1.1	0.9	1.4
K_2O	1.1	1.0	3.0	3.7	3.3	1.7
Na_2O	0.7	0.2	0.8	1.2	1.2	0.6
LOI	10.9	5.5	5.3	3.7	4.0	1.9
Fineness (% retained on 45 μm sieve)	20.6	8	9.5	26.2	29.8	11.6

The fly-ashes (FA) used within the current study were obtained from power stations using anthracitic/bituminous coals. Their oxide analysis is presented in Table 1. For the pozzolanicity studies, the following standard, base-mix formulation was used: samples were prepared by dry-mixing fly-ash and reagent grade calcium hydroxide in the ratio 4:1 and then mixing with distilled water at a water:solids ratio of 0.5. In addition to the base-mix, sodium sulphate (Na_2SO_4), at a dosage of 10g/100g water (0.7Moles/l) was used. The paste samples were contained in the 5×5×5cms cell; the tops of the samples were covered before placing in a temperature controlled cabinet at ambient temperatures of 20°C, 37°C and 54°C (±1°C).

For the frequency-effect studies a CEM I 42.5N cement [6] was used throughout and specimens comprised cement-pastes, mortars and concretes. Cement pastes were prepared using a fly-ash replacement levels of 0%, 10%, 25% and 40% with a water/binder ratio = 0.3. A BS EN 196-1 mortar [7] was used which had a 3:1 sand:binder ratio and a water:binder ratio = 0.5; a CEN reference sand [7] was used and the binder comprised CEM I cement and CEM I cement partially replaced with 33% (by mass) of fly-ash. The concrete mixes used are presented in Table 2 and also had fly-ash replacement levels of 0%, 10%, 25% and 40%. A 10dm^3 planetary motion mixer was used in the preparation of paste and mortar samples and a 0.1m^3 pan mixer was used in the preparation of concrete samples.

Table 2: Summary of cement-paste and concrete mixes studied.

Mix	CEM I kg/m^3	FA kg/m^3	Fine (<4mm) kg/m^3	Coarse kg/m^3		Water l/m^3
				10mm	20mm	
C1	405	-	608	406	811	183
C2	363	40	605	403	806	181
C3	300	100	600	400	800	180
C4	237	158	593	395	791	178

3. Results and discussion

This experimental program focusses on the use of electrical property measurements, obtained using EIS, in the study of fly-ash based systems. Results are presented to highlight the direct application of electrical property measurements in the evaluation of the pozzolanic reactivity of fly-ash through chemical and thermal activation and show the influence of the unburnt carbon within the ash on electrical response.

3.1. Pozzolanicity studies

The bulk resistance, R_b, of the specimens (obtained at 10kHz) was converted to conductivity, σ, through the relationship,

$$\sigma = \left(\frac{L}{R_b A} \right) \text{ Siemens/cm (S/cm)} \quad (2)$$

where A is the area of the electrodes (=5×5 cm^2) and L is their spacing (=4.4cm). The conductivity of the mixture will be dependent upon the fractional volume of aqueous phase; the continuity and tortuosity of the interstitial aqueous path between the electrodes, and the ionic concentration within the aqueous phase; hence, as the mixture reacts and increases in rigidity, all these factors will be affected which will, in turn, change the conductivity of the mixture.

For illustrative purposes, Fig. 2(a) displays the conductivity versus time response for the base-mix using, in this instance, FA2 and for clarity, measurement points have been omitted. The conductivity decreases by approximately 15% over the initial 2-days and remains virtually constant over the remainder of the test period. This would indicate a very sluggish reaction between the fly-ash particles and lime with little strength development; regarding the latter, this was the case as samples could easily be crushed by hand and would agree with published work [8]. Fig. 2(b) presents the conductivity response for all ashes using Na_2SO_4 in the gauging water. It should be noted that the conductivity of these mixtures is almost an order of magnitude higher than their base-mix counterpart values due to the increased ionic content within the gauging water. All curves now display a central region where there is a reduction in conductivity which would signify an increase in rigidity of the mixture, although the time at which this decrease occurs, the time-scale over which the central region occurs, and the rate of the decrease of conductivity are different for each material. These features could be used to quantify the pozzolanic reactivity of each ash; moreover, the derivative of the conductivity/time curves (i.e. dσ/dt) could be considered as indicative of reaction kinetics, hence microstructural development [3].

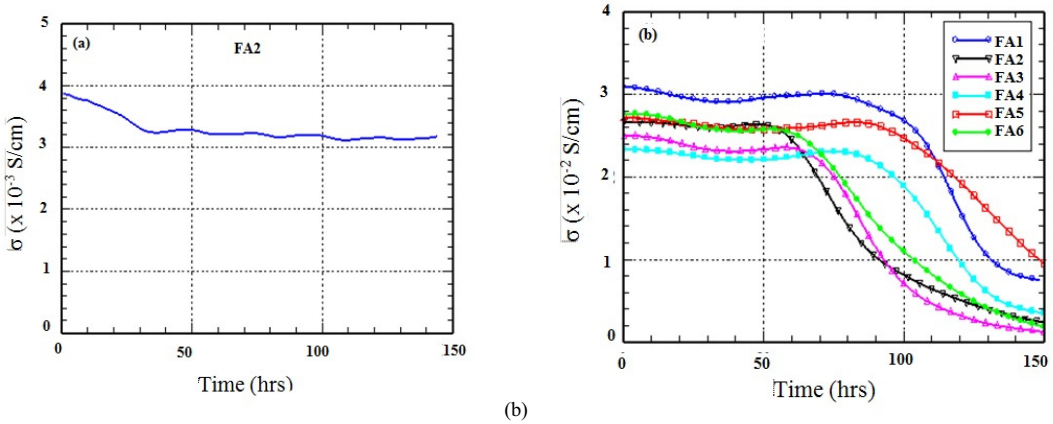

(a) (b)

Fig. 2. Change in conductivity for (a) base-mix with FA2, and (b) base-mix with Na_2SO_4 dissolved in gauging water.

Fig. 3 presents the conductivity/time response for FA4 and the resulting dσ/dt curve. Four regions can be identified: Region I, from initial gauging up to approximately 75 hours, over which time dσ/dt displays minor fluctuations, perhaps indicating some initial chemical activity; Region II, from 75-113 hours, representing an acceleratory period with more rapid chemical activity and is taken to signify stiffening of the mixture; Region III, from 113-145, representing a deceleration period and indicating a reduction in intensity of chemical activity; this leads into Region IV, where there is a more gradual decrease in conductivity over the remainder of the test period. Parallels can be drawn with calorimetry methods used to follow the hydration of Portland cement comprising a dormant period, an acceleratory period, a deceleration period followed by a diffusion controlled period.

A number of metrics can be identified form the electrical responses presented in Figs. 2(b) and 3 which could quantify the pozzolanic reactivity of a particular fly-ash. For example, Table 3 presents,

(a) the extent and duration of Region II; the shorter the duration of Region II, the more reactive the fly-ash;
(b) the ratio σ_o/σ_{150} where σ_o and σ_{150} are, respectively, the values of conductivity at the beginning and end of the test period (i.e. at 150 hours); this ratio would give a semi-quantitative measure of the increase in *rigidity* of the specimen, with increasing rigidity reflected by increasing values of σ_o/σ_{150}.
(c) the maximum value of the derivative, $|d\sigma/dt|_{max}$, which would increase with increasing reactivity of fly-ash; and,
(d) the time, T, to the maximum value of $|d\sigma/dt|$; as with (a) above, the shorter the time, T, the more reactive the fly-ash.

It is evident that there is a good correlation between the values presented in Table 3 and the fineness/coarseness of the ash.

A limited study was undertaken on the influence of ambient temperature on reaction kinetics. Fig. 4 presents the response for FA3 using the base-mix with Na_2SO_4 dissolved in the gauging water; in this Figure, the change in conductivity, σ, relative to the value at the start of the, σ_o, is presented. This Figure clearly indicates that the reaction process is also thermally activated with increasing temperature reducing the time zones over which Regions I-IV start/end.

Table 3. Summary of derivative data for fly-ashes (at 20ºC)

Ash	Extent (duration) of Region II (hrs)	σ_o/σ_{150}	$\lvert d\sigma/dt\rvert_{max}$ ($\times 10^{-4}$ S/cm.hr)	Time, T, to $\lvert d\sigma/dt\rvert_{max}$ (hrs)
FA1	75-117 (42)	4.11	5.3	117
FA2	48-73 (33)	11.07	6.2	73
FA3	57-85 (28)	20.28	6.2	85
FA4	75-113 (38)	6.70	5.4	113
FA5	81-130 (49)	2.89	3.5	130
FA6	50-82 (32)	14.86	4.7	82

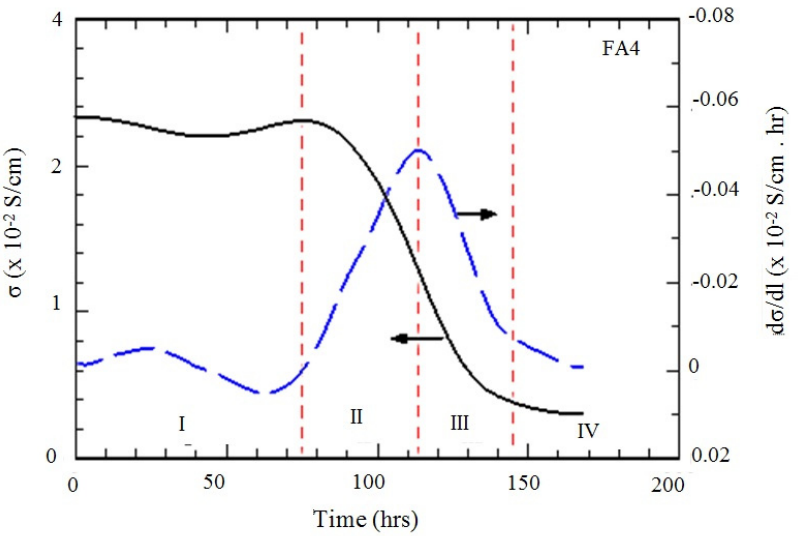

Fig. 3. Change in conductivity for FA4 in Fig. 2(b) and its derivative, dσ/dt.

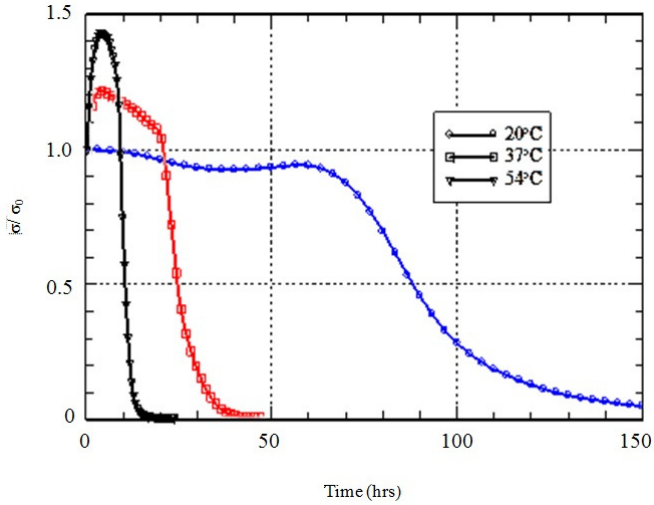

Fig. 4. Relative change in conductivity for FA3 at different ambient temperatures.

3.2. Frequency effect studies

Fig. 5(a) and (b) displays, respectively, the Nyquist plot for mortar samples obtained ~20 minutes after gauging and ~3 days after gauging, with data presented within the frequency range 100Hz-10MHz. For clarity only selected measurement points are highlighted, although plots are drawn through all measurement points. A plain CEM I cement mortar and CEM I mortars with FA2, FA3 and FA6 ashes are presented; some salient frequencies are indicated on these plots.

The plot for the plain cement mortar displays a typical two-region response which is well documented [4], with the electrode polarization arc forming the right-hand-side of a 'V' shaped plot, and a small arc forming the left-hand-side representing the bulk (sample) response. This feature is more evident in Fig. 5(b). The addition of fly-ash results in several significant changes in the Nyquist plot:

i) the two regions associated with the plain mortar response become separated by a distinctive *plateau* region creating a response which is now characterised by three distinct zones: the electrode response, a *flat* region associated with the inclusion of fly-ash, and a bulk arc;
ii) the addition of fly-ash results in an overall displacement of the Nyquist plot to the right; and,
iii) the different fly-ashes produce detectable differences; for example, FA2 displays a distinct plateau region, which takes the form of a circular arc whose centre is depressed below the real axis; FA3 also displays a circular arc, but the extent of the *plateau* region is reduced in comparison to FA2; FA6, although having similar resistances to FA3, displays a plateau region which is not as prominent or *arc-shaped* as FA2 or FA3.

Fig. 5(b) also illustrates the persistence of the effect of the fly-ash even after the cement component has set and entered the hardening process. Regarding (iii) above, this feature is more clearly seen in Fig. 6(a) whereby the Nyquist plots in Fig. 5(a) are *normalized* by dividing both $Z'(\omega)$ and $Z''(\omega)$ by the respective value of bulk resistance (R_b) obtained at the junction between the electrode arc and sample response [9]. This allows a better comparison between the three different ashes as there will be minor variations in the pore fluid chemistry (hence bulk resistance) resulting from differing oxide compositions. Regarding their composition, the most significant difference between these three ashes lies in their carbon content, which is quantified by their LOI. FA2 and FA3 have similar LOI's (5.5% and 5.3% respectively) hence a similar response as shown in Fig. 6(a); however, FA6 is approximately 60% less (1.9%). The electrically conductive nature of the unburnt carbon [9] would explain the reason as to why the plateau region is not as prominent in FA6. It is also interesting to note that this plateau region between the electrode

spur and the bulk arc has been identified in fibre reinforced cement composites containing (electrically conductive) carbon/steel fibres [10−11]. Fig. 6(b) shows the cellular morphology to unburnt carbon in fly-ash.

Fig. 7(a) and (b) present the Nyquist plots taken ~20 minutes after mixing for, respectively, neat cement pastes and concretes with different fly-ash replacement levels (FA2 used in this set of tests). This further highlights the influence of the fly-ash on the electrical response with the plateau region increasing almost in direct proportion to the fly-ash content. The Nyquist plots also become more progressively displace to the right as the samples become more resistive and would imply that the fly-ash is acting as an inert filler at this early stage in the hydration process.

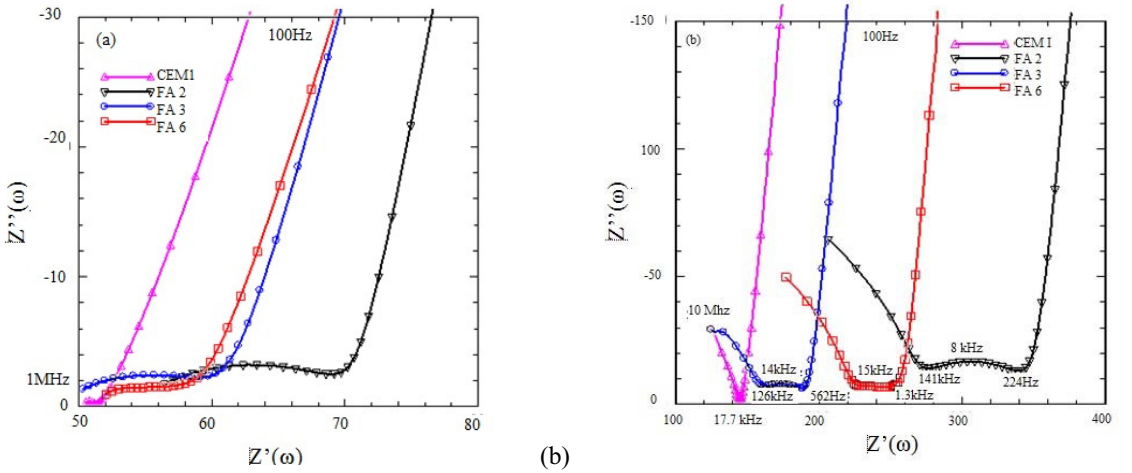

(a) (b)

Fig.5. Nyquist plots for mortars (a) 20 minutes after mixing, and (b) 3-days after mixing.

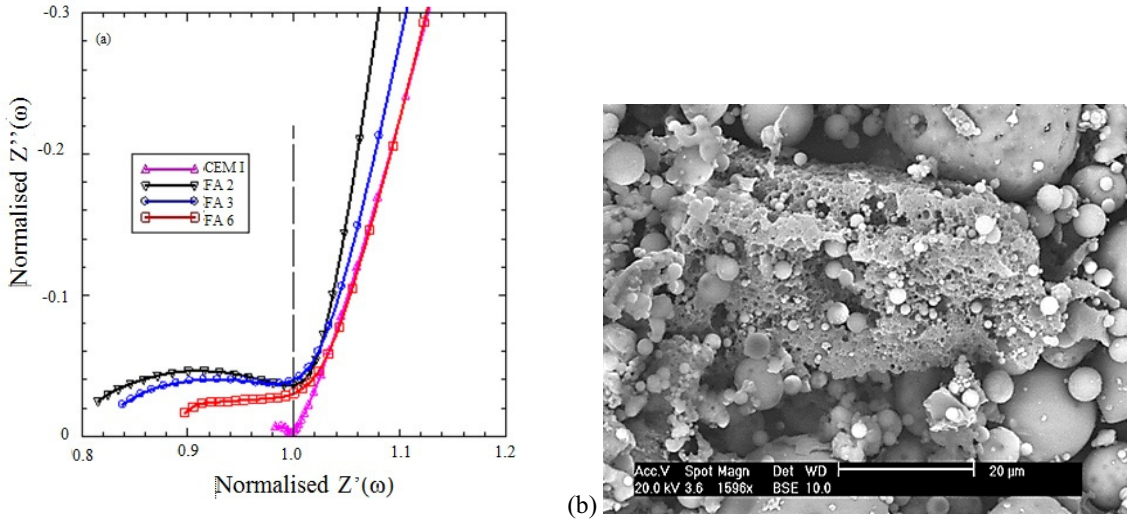

(a) (b)

Fig. 6. (a) Normalised Nyquist plots in Fig. 5(a) allowing comparison of the extent of the plateau region, and (b) micrograph showing cellular nature of unburnt carbon.

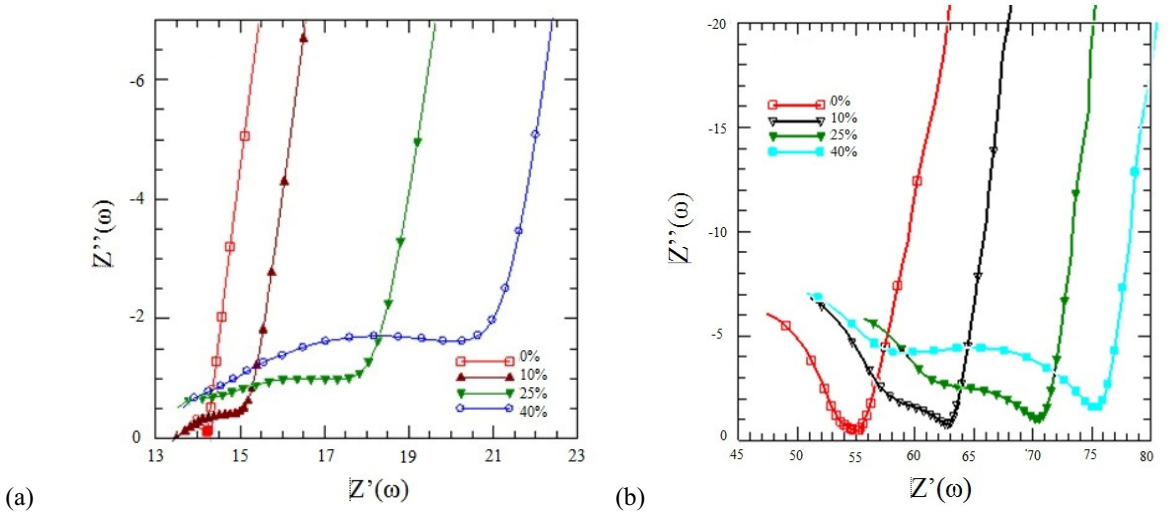

Fig. 7. Nyquist plots for (a) paste and (b) concrete specimens with replacement levels of 0%, 10%, 25% and 40% (FA2).

4. Concluding comments

This paper has extended the range of application of EIS to characterise fly-ash in terms of its unburnt carbon content and reactivity with chemical activators. It was shown that single frequency (10kHz) electricall property measurements could be exploited in following the reaction kinetics – at ambient and elevated temperatures - when FA is activated with a suitable activator or combination of activators; it was found that the fineness of the ash played an important role in this respect. A number of salient features were identified from the conductivity vs. time response and the dσ/dt curve which could be exploited in evaluating the efficacy of different activators. In connection with the unburnt carbon-content of the ash, this results in the emergence of the distinctive plateau when plotted using the Nyquist formalism. As strict requirements are set on the LOI of the ash, EIS techniques could be exploited as a rapid means of quality control in this respect.

Acknowledgements

The authors wish to thank the Engineering and Physical Science Research Council (UK) for financial support.

References

[1] British Standards Institution, BS EN450-1:2012. 'Fly ash for concrete-Part 1: Definition, specifications and conformity criteria', BSI, London.
[2] C. Tashiro, K. Ikeda, Y. Inoue, Evaluation of pozzolanic activity by the electric resistance measurement method, Cem. Concr. Res., 24(6), 1994, pp1133-l139.
[3] W.J. McCarter, D. Tran, Monitoring pozzolanic activity by direct actication with calcium hydroxide, Constr. Build. Matls., 10(3), 1996, pp179-184.
[4] W.J. McCarter, R. Brousseau, The A.C. response of hardened cement paste, Cem. Conc. Res., 20(6), 1990, pp891-900.
[5] W.J. McCarter, H. Ezirim, A.C. Impedance profiling within cover-zone concrete: influence of water and ionic ingress, Advs. Cem. Res., 10(2), 1998, pp57-66.
[6] British Standards Institution, BS EN197-1:2011, Cement: Composition, specifications and conformity criteria for common cements, BSI, London.
[7] British Standards Institution, BS EN 196-1:2005, Methods of testing cement – Part 1: Determination of strength, BSI, London.
[8] C. Kulasuriya, V. Vimonsatit, W.P.S. Dias, P. De Silva, Design and development of Alkali Pozzolan Cement (APC), Constr. Bldg. Matls., 68(15 Oct.), 2014, pp426-433.

[9] W.J. McCarter, T.M. Chrisp, G. Starrs, The complex impedance response of fly-ash cements revisited, Cem. Conc. Res., 34(10), 2004, pp1837-1843.
[10] T.O. Mason, M.A. Campo, A.D. Hixson, L.Y. Woo, Impedance spectroscopy of fiber-reinforced cement composites, Cem. Conc. Comp., 24(5), 2002, pp457-465.
[11] S. Wansom, N.J. Kidner, L.Y. Woo, T.O. Mason, AC-impedance response of multi-walled carbon nanotube/cement composites, Ibid, 28(6), 2006, pp509-519.